Journal of Fluorine Chemistry 130 (2009) 61–66

Contents lists available at ScienceDirect

Journal of Fluorine Chemistry

journal homepage: www.elsevier.com/locate/fluor

Transport in molten LiF–NaF–ZrF_4 mixtures: A combined computational and experimental approach

Mathieu Salanne [a,b,*], Christian Simon [a,b], Henri Groult [a,b], Frédéric Lantelme [a,b], Takuya Goto [c], Abdeslam Barhoun [d]

[a] UPMC Univ Paris 06, UMR 7612, LI2C, F-75005 Paris, France
[b] CNRS, UMR 7612, LI2C, F-75005 Paris, France
[c] Kyoto University, Graduate School of Energy Science, Department of Fundamental Energy Science, Kyoto 6068501, Japan
[d] Université Abdelmalek Essaâdi, Faculté des Sciences, LPCIE, 93000 Tétouan, Morocco

ARTICLE INFO

Article history:
Received 12 March 2008
Received in revised form 16 June 2008
Accepted 3 July 2008
Available online 12 July 2008

Keywords:
Molten salt
Fluorozirconate
Molecular dynamics
Diffusion coefficients
Electrical conductivity

ABSTRACT

The transport properties of several LiF–NaF–ZrF_4 mixtures have been determined. Our work primarily consisted in the determination of the electrical conductivity from experimental measurements and from computer simulations. A good agreement was observed between both approaches. The simulations are based on the molecular dynamics technique and they employ a polarizable interaction potential, which was parameterized from first-principles calculations only. The diffusion coefficients were also determined from the simulations, which allowed us to understand the mechanisms responsible for the variations of electrical conductivity with temperature and composition of the melt.

1. Introduction

Among the nuclear reactors of tomorrow, the molten salt reactor (MSR) has some very specific features from the chemist point of view. While the other reactors would consist of a solid uranium-based fuel inside a primary coolant (water, liquid sodium, helium), in the MSR the fuel is *dissolved* in the molten salt; thus the molten salt is both used as a fuel and as a coolant [1]. Because of this particularity, it is possible to use the MSR reactor either in a thorium/uranium or in an uranium/plutonium fuel cycle. The speciation of all ions will greatly influence a lot of thermochemical properties; for example the nature of majority species is important in determining the solubility of heavy metals, and especially of actinide cations. It is then necessary to understand the short-range structure of the species involved in the foreseen molten salts. Transport of heat and matter also varies a lot from a molten salt to another and it is important to quantify it precisely.

In such liquids, the short-range structure can be probed by many spectroscopic techniques. In molten fluorides, Raman [2] as well as classical NMR or EXAFS [3–9] studies have recently been undertaken by several groups, and proved to be efficient in determining the cationic environments in a wide range of melt compositions. On the contrary, matter transport is difficult to quantify with precision. The NMR gradient field technique was applied to determine diffusion coefficients in a variety of room-temperature ionic liquids [10,11], but it is of course difficult to set up such experiments within the framework of high-temperature, corrosive liquids. An advantage of molten salts is that they consist of charged species only; measuring the charge transport is thus an efficient way to estimate the diffusive properties of the ions. It is indeed possible to measure the electrical conductivity of a molten salt. In the specific systems consisting of molten fluorides, these experiments are very difficult to set up because of the important reactivity of these melts towards oxide glasses. To overcome this difficulty, an electrochemical cell, based on pyrolytic boron nitride, was developed by Hives and Thonstad [12], who used it successfully to measure electrical conductivities of aluminium-based molten fluorides.

From the theoretical point of view, molecular dynamics (MD) simulation is a method aimed in obtaining the microscopic properties of condensed matter, which has proved to be useful in modeling many molten salts. It is notably capable to determine a variety of transport properties. *Individual* properties like the

* Corresponding author at: UPMC Univ Paris 06, UMR 7612, LI2C, F-75005 Paris, France. Tel.: +33 144273265.
E-mail address: mathieu.salanne@upmc.fr (M. Salanne).

0022-1139/$ – see front matter © 2008 Elsevier B.V. All rights reserved.
doi:10.1016/j.jfluchem.2008.07.005

diffusion coefficients are straigthforward to extract, but the *collective* ones like the electrical conductivity and the ion mobility (which measures the displacement of a given species relatively to another one) can also be determined provided that sufficient statistics have been collected [13]. The atomistic representation of the sytems allows to examinate the relationships between these transport quantities and the structure of the melt. In a recent work, we could adress this point in the molten mixtures of LiF with BeF_2 [14–16]. In these melts, the fluidity changes greatly due to the formation of a fluoroberyllate network when the concentration in BeF_2 is increased. The Li^+ ions migration decouples from the other species, and the formation of "migration channels" could be observed.

In the preceding paper [17], we have shown how it is possible to build a polarizable interaction potential for mixtures of LiF, NaF, KF and ZrF_4 from a purely first-principles basis. The accuracy of the simulations was checked by computing heat-transfer properties, like the heat capacities and the viscosities, which compared satisfactorily with experimental measures, for two different salts (LiF–NaF–KF and NaF–ZrF_4 mixtures). The objective of present work is to determine transport properties of such melts. In order to get a first experimental information for these quantities, we have performed electrical conductivity measurements in mixtures consisting in LiF, NaF and ZrF_4. Systems with the same compositions have also been studied by MD simulations. The ratio of alkali cations Li^+/Na^+ was almost kept constant while the concentration of ZrF_4 was varied from 0 to 29 mol% to study the importance of heavy cations incorporation on the matter and charge transport. These melts have been chosen because Zr^{4+} is a good example of highly charged cations, and it is easier to handle than actinide species like Th^{4+} or U^{4+}. In this paper we will first consider the values for the electrical conductivity from both the experimental and the theoretical approach, then we will focus on the diffusive properties of the various species, with a particular emphasis on the role of ZrF_4 concentration.

2. Results and discussion

2.1. Electrical conductivities

2.1.1. Measurements

Impedance measurements at ocp (open circuit potential) were conducted to follow the variation of the electrolyte resistance versus temperature. As an example, the Nyquist diagrams obtained for different temperatures of the eutectic mixture LiF–NaF–ZrF_4 (29 mol% of ZrF_4) are given in Fig. 1. The electrolyte resistance is obtained at $-\Im(Z) = 0$. As clearly shown on this figure, the electrolyte resistance decreases with increasing temperature. Taking into account the cell constant and the resistance values deduced from the impedance spectra, we could determine the experimental conductivities for three different compositions of the molten fluoride mixtures.

The corresponding experimental points are shown on the top panel of Fig. 2. The three compositions are given on the same figure in order to underline the variation of electrical conductivity with the amount of ZrF_4 in the molten salt. The lines correspond to Arrhenius fits to the data. Electrical conductivity of the LiF–NaF eutectic mixture has already been measured and the results are reported in Ref. [18]. A small difference was observed here, and we obtained slightly lower values. This difference is mostly due to the relative incertitude in these experiments; as it was shown in several recent reports [19] all the physico-chemical properties are difficult to measure precisely in these media, but the principal interest is to be able to compare several systems one with each other in order to select the best compromise between all the competing properties.

The first observation is the important diminution of electrical conductivity when ZrF_4 is added to the melt. Such a behavior has already been observed when adding BeF_2 to LiF: in these melts, the

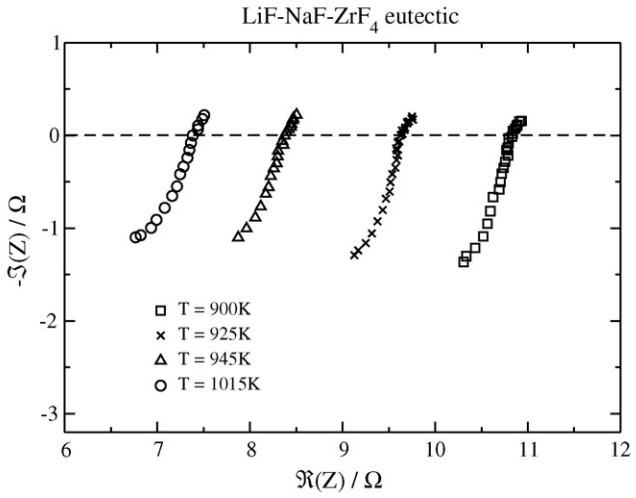

Fig. 1. Nyquist diagrams obtained at different temperatures for the LiF–NaF–ZrF_4 eutectic (29 mol% ZrF_4) at various temperatures. The electrolyte resistance is obtained at $-\Im(Z) = 0$.

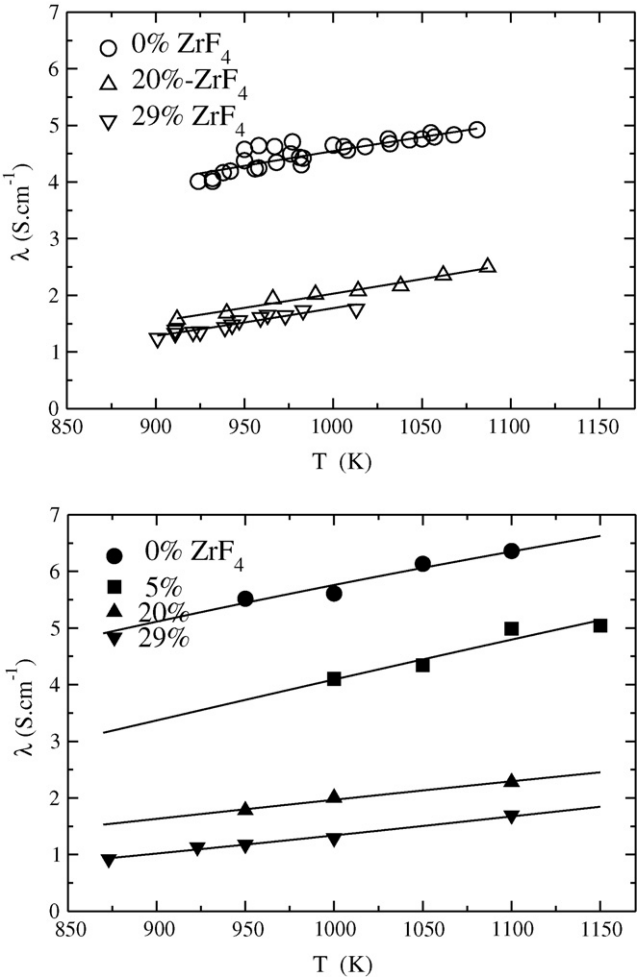

Fig. 2. Experimental (top) and simulated (bottom) values for the electrical conductivity as a function of temperature for all the compositions studied.

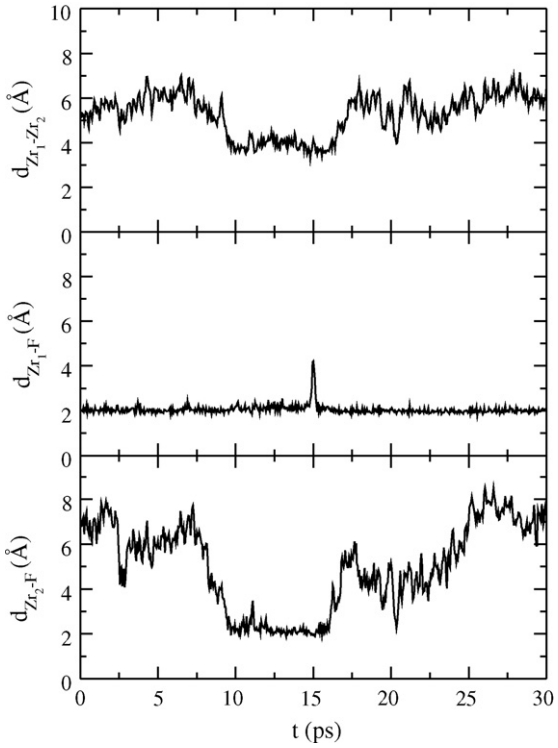

Fig. 3. Distances between one F^- and two different Zr^{4+} ions as a function of time during a molecular dynamics simulation.

progressive formation of fluoroberyllate species, which have relatively small diffusion coefficients, provokes the diminution of electrical conductivity [15,16]. The diminution is not as strong as the corresponding increase in the viscosity, and this decoupling was associated to the important contribution of Li^+ions in the overall conductivity. In the case of ZrF_4 containing melts, Raman spectroscopy studies showed evidence for the formation of small size fluorozirconate chains [2], and the same effects can thus be expected. At this point molecular dynamics (MD) simulations can provide us a useful picture of that process. In this method, the molten salt is simulated at the atomic scale and trajectories of several nanoseconds are generated for all the ions of a given condensed phase system (through the use of periodic boundary conditions). Fig. 3 displays the variation of the distances between one F^- and two different Zr^{4+} ions as a function of time during a MD simulations. For the whole period of time represented, the F^- ion stays in the first solvation shell of the first Zr^{4+}, the distance between them slightly fluctuating around a value of 2 Å. Then, between $t \approx 10$ ps and $t \approx 15$ ps, the F^- also is in the solvation shell of the second Zr^{4+} ion, in a so-called bridging position. The distance between the two cations then fluctuates around 4 Å. Therefore, the MD simulations support the formation of some complex fluorozirconate species in the melt, which are responsible for the diminution of the electrical conductivity when the ZrF_4 concentration increases.

The Arrhenius fits allow a better understanding of the variation of electrical conductivity with temperature. We obtained activation energies of respectively 9.3, 20.8 and 24.2 kJ mol^{-1} for the 0, 20 and 29 mol% ZrF_4 containing mixtures. This increase can again be associated with the variation of the structure of these molten salts: because of the high association of Zr^{4+} and F^- ions, the diffusion of all the species will involve jumps across higher potential barriers. When the temperature is increased, such jumps will become more and more frequent. Thus, for the LiF–NaF mixture, the electrical conductivity will already be high at low temperatures because of the small potential barrier, and it will slowly increase with temperature, while in the ZrF_4 containing melts, the charge transport will be slow at low temperature when the ions have difficulties to jump across higher potential barriers, but it will increase faster when their motion will become easier.

2.1.2. Simulations

During the MD simulations, sampling of several quantities like the energies, velocities or the displacements was performed periodically. The electrical conductivity is calculable as an integral over the charge current correlation function [20]:

$$\lambda = \frac{\beta e^2}{V} \int_0^\infty J(t)\, dt \tag{1}$$

where $\beta = (1/k_B T)$, k_B is the Boltzmann constant, e is the electronical charge, V is the simulation cell volume and J is defined as

$$J(t) = \sum_{i,j}^{N} q_i q_j \langle \vec{v}_i(t) \vec{v}_j(0) \rangle \tag{2}$$

$$J(t) = \sum_{i}^{N} q_i^2 \langle \vec{v}_i(t) \vec{v}_i(0) \rangle + \sum_{i,j \neq i}^{N} q_i q_j \langle \vec{v}_i(t) \vec{v}_j(0) \rangle \tag{3}$$

with q_i and $\vec{v}_i$ the charge and velocity of each ion. The conductivity therefore involves the relative motion of all species. It is convenient to re-express the conductivity in the form of a mean-squared displacement [21], this expression is

$$\lambda = \frac{\beta e^2}{V} \lim_{t \to \infty} \frac{1}{6t} \left\langle \left| \sum_{i}^{N} q_i \delta \vec{r}_i(t) \right|^2 \right\rangle \tag{4}$$

$$\lambda = \frac{\beta e^2}{V} \lim_{t \to \infty} \frac{1}{6t} \left\langle \left| \sum_{\alpha}^{N_\alpha} q_\alpha \vec{\Delta}_\alpha(t) \right|^2 \right\rangle \tag{5}$$

where $\vec{\Delta}_\alpha(t) = \sum_{i \in \alpha} \delta \vec{r}_i(t)$ is the net displacement of all the ions of species α in time t.

As outlined above, the displacements of each ion are periodically sampled during the simulation, and the electrical conductivity can thus be calculated from the slope of the corresponding average of mean-squared displacements versus time, which become linear after the short-time correlations have disappeared. It is indeed a collective quantity, and such a calculation involves very long simulation runs.

The calculated electrical conductivities for the four mixtures (0, 5, 20 and 29 mol% of ZrF_4, in molar percent) at different temperatures are given in Fig. 2. The agreement with corresponding experimental data is good: for the LiF–NaF mixture, simulation values are higher than the experimental ones, but as it was underlined earlier a slight difference was obtained with previous study on that mixture [18]. Agreement between simulation values and Janz data is better, and this results confirm the fact that relatively important uncertainties have to be accounted when performing physical chemistry measurements in molten fluorides. In the two concentrated ZrF_4 melts, the agreement between simulation and experiment is good, with a slight underestimation of electrical conductivity in the simulation of the 29 mol% ZrF_4 mixture. This confirms that our model is able to reproduce transport properties of molten fluorides; such a validation had already been shown in the case of LiF–BeF_2 mixtures in Ref. [15]. In the preceding paper [17], we could show that the heat-transfer properties, which include another transport coefficient, the viscosity, are also very well reproduced. We can then conclude

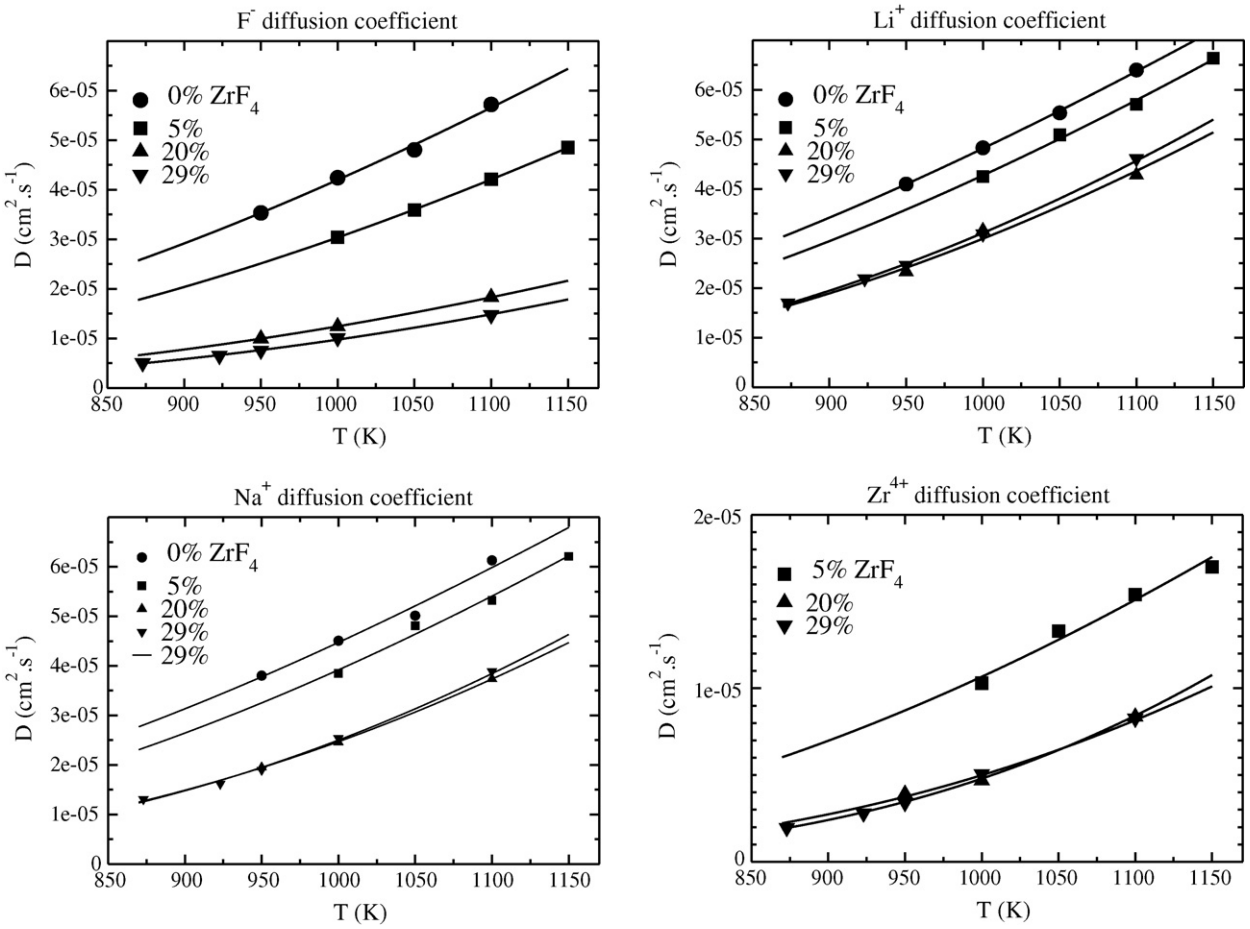

Fig. 4. Variations of the diffusion coefficients with temperatures for all the species and concentrations studied.

that the MD simulations undertaken give a good description of the physical chemistry of the system, and that it will provide a very reliable estimation of the diffusion coefficients, for which no experimental data is available.

2.2. Diffusion coefficients

MD is a powerful tool to obtain collective quantities like the electrical conductivity, but it is even more efficient in determining individual quantities like the diffusion coefficients of the various species. A precise experimental determination of this quantity is difficult to realize and requires for example the use of advanced NMR spectroscopy techniques. It is routinely performed in room-temperature ionic liquids [10,11], but up to now no such study appeared for molten fluorides. Estimates can be done from electrochemical measurements, and for example a value of 2.92×10^{-5} cm^2 s^{-1}was determined for the diffusion coefficient of Zr^{4+}present in small concentration in a LiF–NaF mixture at 1010 K [22]. In MD simulations, the diffusion coefficient can also be computed from the mean-squared displacements through the Einstein expression:

$$D_\alpha = \lim_{t\to\infty} \frac{1}{6t} \langle |\delta \vec{r}_i(t)|^2 \rangle \quad (6)$$

Here, the mean-squared displacements are averaged over all the ions for a given species, thus the diffusion coefficient is an individual property, unlike electrical conductivity. Statistics for this quantity are then much better in a MD simulation run. The diffusion coefficients are plotted versus temperature for all the ions in Fig. 4.

Like the electrical conductivity, the diffusion coefficients of all the ions tend to decrease when ZrF_4 is added to the melt. In Fig. 5 are reported the variations of the diffusion coefficients for all the species versus ZrF_4 concentration at a given temperature of 1000 K. In the LiF–NaF system, the various species diffusion coefficients

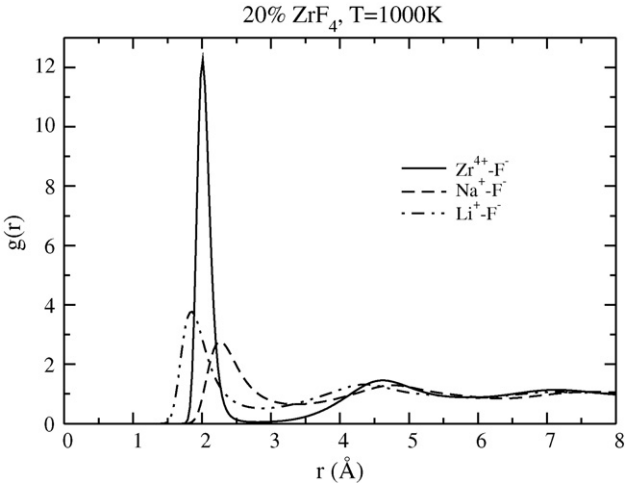

Fig. 5. Cation anion radial distribution functions for the 20 mol% ZrF_4 melt at a temperature of 1000 K.

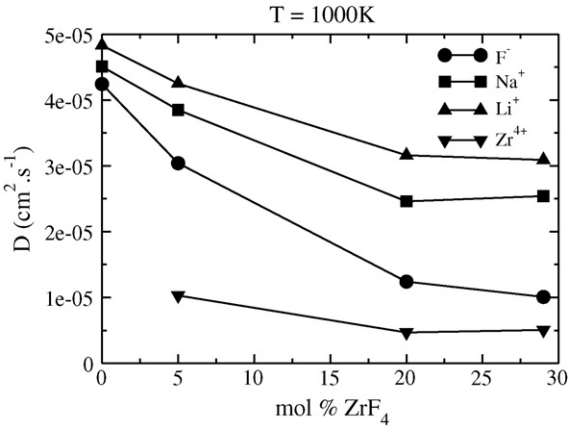

Fig. 6. Variation of the diffusion coefficients of all the ions with ZrF_4 concentration, for a constant temperature of 1000 K.

are almost similar. When ZrF_4 is added to the melt, the Li^+ and Na^+ diffusion coefficients suffer a slight diminution, while the F^- one decreases significantly. The origin of this behavior can be traced in the solvation shells of the cations. The cation anion radial distribution functions (RDF) are plotted for the 20 mol% ZrF_4 melt in Fig. 6. Two very different patterns are observed: the first RDF peak for the Zr–F pair is very sharp, with a high maximum and a very low minimum (nearly 0), whereas, for the Li–F and Na–F pairs, this peak is much broader and its minimum is quite high, suggesting relatively rapid exchange of coordinated F^-ions with the bulk. The shape of the Zr–F RDF suggests some much longer residence times for the F^-ions in the Zr^{4+} solvation shells, which is confirmed by an examination of the variation of the distance between the first Zr^{4+} and the F^- ion with time in Fig. 3. Therefore, in a ZrF_4-containing melt, one can distinguish the "free" F^- ions from the linked ones. When the ZrF_4 concentration increases, so will behave the linked/free ratio. On the dynamic point of view, this causes D_{F^-} to reach similar value as $D_{Zr^{4+}}$, as observed in Fig. 4.

An interesting feature appears upon examination of the variations of diffusion coefficients of the three cations with temperature. In Fig. 4, one can see that all species diffusion coefficients are smaller for the 29 mol% ZrF_4 melt than in the 20 mol% ZrF_4 one at low temperatures, but they become greater for the highest temperature studied, i.e., 1100 K. This is directly related to the variation of activation energies already discussed for the electrical conductivities. Similarly to the electrical conductivities, activation energies for the diffusion coefficients determined from the Arrhenius fits (given by the lines in Fig. 4) increase with the ZrF_4 proportion. In the 29 mol% mixture, the diffusion is more activated with temperature than in the 20 mol% one, which results in the observation of a crossing point in the diffusion coefficients of the cations. This is not true for F^- ions because this effect is hidden by the important diminution of their diffusion coefficients due to their association with Zr^{4+} ions.

2.3. Validity of the Nernst–Einstein relationship

The expression 4, which was used to determine the conductivity, can be approximated by neglecting the correlations between the displacements of different ions, i.e.,

$$\langle \delta\vec{r}_i(t)\delta\vec{r}_j(t)\rangle = 0, \quad i \neq j \tag{7}$$

This leads to the Nernst–Einstein approximation, where the electrical conductivity (written λ^{NE}) is directly proportional to the diffusion coefficients:

$$\lambda^{NE} = \beta e^2 V \sum_{i\in\alpha} \rho_i q_i^2 D_i \tag{8}$$

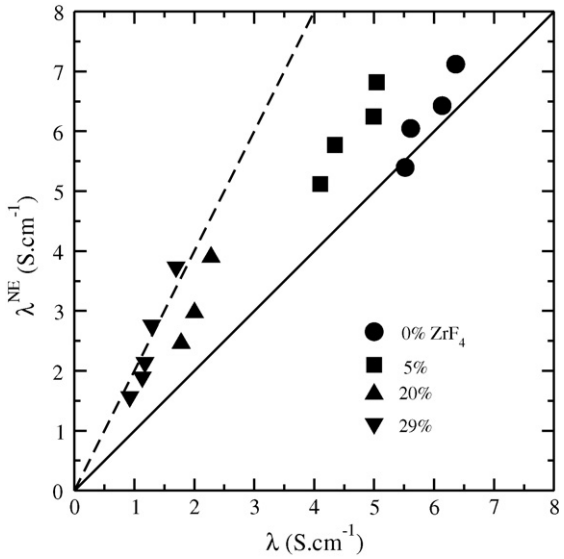

Fig. 7. Electrical conductivity as approximated by the Nernst–Einstein relationship, λ^{NE}, vs. the real electrical conductivity λ (MD simulations values). The diagonal solid line corresponds to the equation $\lambda^{NE} = \lambda$, while the dashed line corresponds to the equation $\lambda^{NE} = 2 \times \lambda$.

In this expression ρ_i is the number density of species *i*. These Nernst–Einstein conductivities have been computed and are compared to the conductivities determined without any approximation on Fig. 7. We can see that the approximation gives reasonable results for the LiF–NaF mixture (because the data points are close to the solid line, which corresponds to the equation $\lambda^{NE} = \lambda$), but strong deviations are observed for ZrF_4 containing systems (points appear closer to the dashed line, which corresponds now to $\lambda^{NE} = 2 \times \lambda$, when the ZrF_4 concentration increases). In fact, Nernst–Einstein is known to be accurate in ion containing liquids with negligible association between distinct ions like the diluted aqueous electrolytes. This shows again that association effects are very important in the ZrF_4-containing systems, because of the long residence time of the F^- in the Zr^{4+} ions solvation shell and the formation of small fluorozirconate chains. In such systems, electrical conductivity measurements are not sufficent to estimate precisely the diffusivity of the various species in the melt. Structural informations, that can be provided by MD simulations but also by experimental techniques as the Raman or EXAFS spectroscopy are then necessary to understand the possible association effects.

3. Conclusion

In this study we have shown how a coupled experimental and theoretical strategy can be useful in determining the charge and matter transport properties of molten fluorides consisting in mixtures of LiF, NaF and ZrF_4. The electrical conductivity could be determined by two methods with a satisfactory agreement in the obtained values. The diffusion coefficients of all the ions were determined from the molecular dynamics simulations. Variation of all these transport coefficients with the temperature and the composition of the system were examined, and an interesting analogy with the LiF–BeF_2 was observed. the main characteristics of the diffusion processes are important coupling effects between

the Zr^{4+} and F^- ions, while the alkali ions tend to diffuse rapidly in all the systems.

The agreement between experiment and simulation is important in that it means that both the model chosen, the polarizable ion model, and the procedure used to parameterize the interaction potential, i.e. from first-principles calculations, are consistent with the physical chemistry of the molten fluoride liquids. In the framework of the MSR and other molten salts using nuclear reactors, many species like the actinides, lanthanides or fission/corrosion products will have to be considered, and it would be very difficult to perform spectroscopic investigations and thermodynamic studies for every composition of interest. MD therefore appears as an interesting alternative to fill the gaps in the databases necessary in the perspective of the setup of these reactors concepts.

Future theoretical work should focus on interaction potential development for many other species including lanthanide and actinide cations. However it is of primary interest to continue to confirm the validity of the computed physico-chemical properties, and in molten salts the measurement of the electrical conductivity is a method of choice for this task because it gives direct information on the transport of matter.

4. Experiments

4.1. Electrical conductivity measurements

4.1.1. Salts

LiF, NaF, KF and ZrF_4 powders provided by (Sigma–Aldrich) were treated under fluorine atmosphere to remove traces of oxides or hydroxides and stored in a glove box (water content: 5 ppm) under Ar atmosphere. Then, the constituents were dried before each experiment under vacuum at 150 and 250 ° C during 1 day for each step. Then, the fluorides mixture were introduced in the reactor and dried again at 150 ° C under vacuum during 1 day and then heat-treated very slowly up to the required temperature (ramp: 5 °C). the impedance measurements were done about 1 h after the stabilisation of the temperature. Whatever the electrochemical tests, all measurements were performed under argon atmosphere. The temperature of the molten salt was controlled using a chromel–alumel thermocouple.

4.1.2. Measurements

The conductivity cell was derived from the one proposed by Hives and Thonstad [12]. Briefly, the cell consists of a pyrolytic boron nitride tube (inner diameter of 5.9 mm and length of 90 mm) and a graphite crucible used as one electrode. A tungsten rod used as the second electrode was introduced in the boron nitride tube. The graphite crucible contains about 20 g of salt. The cell was placed in a cell made of an outer stainless steel envelope. The measurement were done under Ar atmosphere. The resistance of the molten salts was deduced from electrochemical impedance measurements (Solartron 1260). The ac amplitude of the signal was 10 mV and the frequency range was comprised between 100 kHz and 1 Hz. Three successive diagrams were recorded to ensure the reproducibility of the measurement. The cell constant ($\approx 13\ cm^{-1}$) was determined by calibration of the cell using LiCl–KCl eutectic (58.8–41.2 mol%) between 690 and 890 K.

4.2. Molecular dynamics simulations

Four different compositions of LiF–NaF–ZrF_4 mixtures have been studied by molecular dynamics simulations. The number of atoms involved in the simulation cells are detailed in Table 1. The interaction potential used in those simulations is a "polarizable ion model", which consists of the sum of pairwise additive interactions supplemented with a many-body polarization term. Its form and values for all the parameters necessary are given in the preceding paper [17]. The parameters were determined from a purely first-principles basis, so that no experimental data but the density of pure compounds have been used in that procedure.

Table 1
Number of ions of each species in the simulation cells

LiF–NaF–ZrF_4 composition	N_{F^-}	N_{Li^+}	N_{Na^+}	$N_{Zr^{4+}}$
61–39–0 (A)	216	132	84	0
58–37–5 (B)	260	132	84	11
47–33–20 (C)	282	84	58	35
42–29–29 (D)	374	84	58	58

At all the temperatures studied, the systems were first equilibrated in the *NPT* ensemble with a pressure fixed at 0 GPa. We then performed *NVT* runs at the equilibrated cell volume. The method used to enforce canonical (*NVT*) ensemble sampling is the Nosé–Hoover chain thermostat method [23,24]. We chose a time step of 0.5 fs and performed simulations of more than 2 ns for each system in order to collect sufficent statistics to calculate the electrical conductivities of the melts.

Acknowledgements

The authors would like to acknowledge the financial support of PACEN (Programme sur l'Aval du Cycle et l'Energie Nucléaire) through PCR-RSF and GDR PARIS programmes. Pr. D. Avignant (UBP, Clermont-Ferrand) is gratefully acknowledged for his help in salt purification.

References

[1] C.L. Brun, J. Nucl. Mater. 360 (2007) 1–5.
[2] V. Dracopoulos, J. Vagelatos, G. Papathodorou, J. Chem. Soc., Dalton Trans. (2001) 1117–1122.
[3] A. Rollet, C. Bessada, Y. Auger, P. Melin, M. Gailhanou, D. Thaudière, Nucl. Instrum. Meth. Phys. Res. B 226 (2004) 447–452.
[4] A. Rollet, C. Bessada, A. Rakhmatullin, Y. Auger, P. Melin, Comptes Rendus Chimie 7 (2004) 1135–1140.
[5] A. Rollet, A. Rakhmatullin, C. Bessada, Int. J. Thermophys. 26 (2005) 1115–1126.
[6] C. Bessada, A. Rollet, A. Rakhmatullin, I. Nuta, P. Florian, D. Massiot, Comptes Rendus Chimie 9 (2006) 374–380.
[7] C. Bessada, A. Rakhmatullin, A. Rollet, D. Zanghi, J. Nucl. Mater. 360 (1) (2007) 43–48.
[8] S. Watanabe, H. Matsuura, H. Akatsuka, Y. Okamoto, P. Madden, J. Nucl. Mater. 344 (1–3) (2005) 104–108.
[9] S. Watanabe, A. Adya, Y. Okamoto, N. Umesaki, T. Honma, H. Deguchi, M. Horiuchi, T. Yamamoto, S. Nogushi, K. Takase, A. Kajinami, T. Sakamoto, M. Hatcho, N. Kitamura, H. Akatsuka, H. Matsuura, J. Alloys Compod. 408–412 (2006) 71–75.
[10] Y. Saito, K. Hirai, K. Matsumoto, R. Hagiwara, Y. Minamizaki, J. Phys. Chem. B 109 (7) (2005) 2942–2948.
[11] A. Rollet, P. Porion, M. Vaultier, I. Billard, M. Deschamps, C. Bessada, L. Jouvensal, J. Phys. Chem. B 111 (41) (2007) 11888–11891.
[12] J. Hives, J. Thonstad, Electrochem. Acta 49 (28) (2004) 5111–5114.
[13] B. Morgan, P. Madden, J. Chem. Phys. 120 (3) (2004) 1402–1413.
[14] R. Heaton, R. Brookes, P. Madden, M. Salanne, C. Simon, P. Turq, J. Phys. Chem. B 110 (23) (2006) 11454–11460.
[15] M. Salanne, C. Simon, P. Turq, R. Heaton, P. Madden, J. Phys. Chem. B 110 (23) (2006) 11461–11467.
[16] M. Salanne, C. Simon, P. Turq, P. Madden, J. Phys. Chem. B 111 (18) (2007) 4678–4684.
[17] M. Salanne, C. Simon, P. Turq, P. Madden, J. Fluorine Chem. 130 (2009) 38-44.
[18] G. Janz, J. Phys. Chem. Ref. Data 17 (2) (1988) 1–309.
[19] D. Williams, L. Toth, K. Clarno, Tech. Rep. ORNL/TM-2006/12, Oak Ridge National Laboratory, Oak Ridge, TN, 2006.
[20] J.-P. Hansen, I. McDonald, Theory of Simple Liquids, 2nd ed., Academic Press, 1986.
[21] M. Castiglione, P. Madden, J. Phys.: Condens. Matter 13 (44) (2001) 9963.
[22] H. Groult, A. Barhoun, H.E. Ghallali, S. Borensztjan, F. Lantelme, J. Electrochem. Soc. 155 (2) (2008) E19–E25.
[23] S. Nosé, Mol. Phys. 52 (1984) 255–268.
[24] G. Martyna, M. Klein, M. Tuckerman, J. Chem. Phys. 97 (4) (1992) 2635–2643.